

Optimal sensor selection for prediction-based iterative learning control of distributed parameter systems

Maciej Patan^{*}, Kamil Klimkowicz[‡], Krzysztof Patan

14.07.2022

Abstract

The purpose of this study is to develop an effective computational scheme to solve the optimal tracking control problem for repeated trials in distributed-parameter system in the situation where quantity under control cannot be observed directly. In such situations, the reliability of model predictions becomes more important than the accuracy of model parameters, because the ultimate objective in model-based control is the prediction or forecast of the system states. Particularly, given a finite number of possible spatial locations at which sensors may reside, we select gaged sites so as maximize the prediction accuracy. For that purpose, an suitable output criterion is proposed as a measure of the prediction accuracy and the sensor selection problem formulated in terms of optimization task. To solve it, a specialized technique is adopted based on relaxation of the original discrete optimization problem which amounts to operating on the density of sensors in lieu of their individual positions. As a result, a simple and effective exchange algorithm is outlined to select the gaged sites. Then, the measurement schedule providing the most informative system observations is further incorporated into the adaptive control scheme based on iterative learning control technique for effective solution of underlying tracking control problem. The proposed approach is verified by numerical experiments on the model of the friction welding process of two aluminum plates.

1 Introduction

Distributed parameter systems (DPSs) form a wide range of complex real-world processes of a great practical importance. In recent years, due to the constantly growing demands on the control quality for dynamic systems, the strong interest is observed in extending the modeling and control design to

^{*}This research was funded in whole or in part by National Science Centre in Poland, grant No. 2020/39/B/ST7/01487. For the purpose of Open Access, the author has applied a CC-BY public copyright licence to any Author Accepted Manuscript (AAM) version arising from this submission.

[†]M. Patan and K. Patan are with the Institute of Control and Computation Engineering, University of Zielona Góra, ul. Szafrana 2, 65-246 Zielona Góra, Poland. E-mail: {m.patan,k.patan}@issi.uz.zgora.pl

[‡]K. Klimkowicz is with the Institute of Automation, Electronic and Electrical Engineering, University of Zielona Góra, ul. Szafrana 2, 65-246 Zielona Góra, Poland. E-mail: k.klimkowicz@iee.uz.zgora.pl

the framework of spatio-temporal systems. This leads directly to the complex infinite-dimensional mathematical description usually using partial differential equations (PDEs) [2, 4, 9]. Although, more sophisticated level of modeling, the significance of this design has been widely recognized, e.g., in air quality control, fluid dynamics, heat transfer or numerous industrial processes [7, 18, 23, 24, 26, 27]. The existing solutions usually require some extensive and complex computational methods. This discourages their use as in industrial applications a relatively simple implementation is preferred allowing for lower cost and easier maintenance of the control process.

To address this issue, in this work we provide a new results making use of iterative learning control (ILC) which emerged in the context of systems that repeat the same finite duration task over and over again. This form of data-driven repetitive control was first proposed in the mid 80s and since then it has been a very active area of research and applications [1, 3, 5, 6, 12, 17, 25, 29].

However, in the case of repetitive DPSs there is still no general theory for the control synthesis of ILC, despite the fact that such processes are quite frequent in industrial production. A great difficulty here is the inability to provide the simultaneous actuation and sensing action over the entire spatial domain. This leads to the question of how to properly distribute sensing and actuating over the spatial domain so as the information content of the resulting measurements will be sufficient to perform the arbitrarily defined control task. Therefore the contributions to this field are rather limited. Some successful attempts in terms of boundary control for parabolic PDEs were reported in [10, 13, 14] but are dedicated to to one spatial dimension and fixed measurement locations. The ILC for hyperbolic PDEs in multidimensional case based on different type of spatial discretizations were developed in [8, 22] but there are strictly dependent on spatial mesh resolution. Recently, the optimal reference tracking approach has been proposed by the authors based on the concept of distributed sensing and actuation [19, 20] with a decentralized control update strategy.

In many applications, however, the controlled quantity is quite often unavailable for direct measurement what may be a significant impediment to effectively apply the ILC, e.g., when some spatial area is inaccessible to measurement transducers or we have to control the state of the DPS in hand via indirect observations of its output. In such a way, the reliability of model predictions is sometimes more important than the accuracy of model parameters, because the ultimate objective in control and modelling is the prediction or forecast of the system states [15]. The topic was discussed to some extent in [27], but without connection to control of DPS. This gap constitutes the main motivation for the study undertaken here in order to extend approach set forth in [20]. For that purpose, the suitable output criterion related to the variance of the controlled variable as measure of the prediction accuracy is proposed. The setting examined here corresponds to situations where given a finite number of possible spatial sites at which sensors may take observations, we select some subset where the measurements provide the most informative data for the prediction. The resulting discrete optimization problem is then approximated based on relaxation which amounts to operating on the density of sensors in lieu of their individual positions. In particular the Fedorov's idea of directly constrained design measures [11] is used resulting in a simple and effective exchange algorithm being a dedicated adaptation of the techniques reported in [18, 21, 27].

The main contribution of this work is as follows: (1) the proposal of the appropriate criterion to quantify the prediction accuracy, (2) adaptation of the ingenious exchange algorithm for efficient approximation of the solution for sensor selection problem, (3) the extension of the ILC scheme developed in [20] to the prediction-based measurement strategy, (4) verification on the highly non-trivial three-dimensional example of friction welding of two aluminium plates.

2 Sensor selection problem in context

2.1 Model of system and measurements

Let us consider a bounded spatial domain $\Omega \subset \mathbb{R}^d$ with sufficiently smooth boundary Γ , a bounded time interval $T = (0, t_f]$, and a DPS whose scalar state at a spatial point $x \in \bar{\Omega} \subset \mathbb{R}^d$ and time instant $t \in \bar{T}$ is denoted by $y(x, t)$. Mathematically, the system state can be described by PDE

$$\frac{\partial y}{\partial t} = \mathcal{F}(x, t, y, \theta) \quad \text{in } \Omega \times T, \quad (1)$$

where \mathcal{F} is a well-posed, linear, differential operator which involves first- and second-order spatial derivatives and may include terms accounting for forcing inputs specified *a priori*. The equation (1) is accompanied by the appropriate boundary and initial conditions

$$\mathcal{B}(x, t, y, \theta) = u(x, t) \quad \text{on } \Gamma \times T, \quad (2)$$

$$y = y_0(x) \quad \text{in } \Omega \times \{t = 0\}, \quad (3)$$

respectively, \mathcal{B} being an operator acting on the boundary Γ and y_0 a given function. Here, $u(x, t)$ denotes the external control action on the boundary being the result of actuation using R devices. Further, it is assumed to be implemented in the form of a control-affine approximation, i.e.,

$$u(x, t) = \sum_{i=1}^R q_i(x) u_i(t), \quad (4)$$

where $u_i(t)$ is the control signal of the i -th actuator and $q_i(x)$ denotes a spatial distribution of actuation, which is nonnegative integrable function satisfying the normalization condition, i.e. $\int_{\Gamma} q_i(x) ds = 1$. Such actuation field is very convenient as it covers a wide variety of practical situations (from pointwise actuation to fully distributed control).

Conditions (2) and (3) complement (1) such that the existence of a sufficiently smooth and unique solution is guaranteed. We assume that the forms of \mathcal{F} and \mathcal{B} are given explicitly up to an m -dimensional vector of unknown constant parameters θ which must be estimated using observations of the system. The implicit dependence of the state y on the parameter vector θ will be denoted as $y(x, t; \theta)$.

In what follows, we consider the observations provided by the network of n stationary pointwise sensors taking measurements continuously in time in consecutive trials of the process, i.e.

$$z_k^j(t) = y_k(x^j, t; \theta) + \varepsilon_k(x^\ell, t), \quad t \in T, \quad (5)$$

where k is the trial number, $z_k^j(t)$ is the scalar output and $x^j \in X$ stands for the location of the j th sensor ($\ell = 1, \dots, n$), X signifies the part of the spatial domain Ω where the measurements can be made. The control input vector at k th trial is denoted as $\mathbf{u}_k(t) = [u_{k1}(t), \dots, u_{km}(t)]^T$ and the respective system response as $y_k(x, t; \theta)$. Finally, $\varepsilon_k(\cdot, \cdot)$ denotes the measurement noise customarily assumed to be zero-mean, spatially uncorrelated and white Gaussian process [16, 27].

2.2 Iterative learning control

In the setting considered here, the control objective is to modify the input signal vector $\mathbf{u}_k(t)$ in each subsequent trial in order to make the system output $z_k(t)^*$ at some spatial location $x^* \in \Omega \setminus X$ follow some differentiable reference trajectory $\mathbf{z}_{\text{ref}}(t)$ with arbitrary accuracy.

The effect of this procedure is to be able to estimate the value of the point measurement $q(x, t; \theta)$ from the measurement prohibited zone. Such a zone may, for example, be inaccessible to the sensor by being covered with tool elements or by a restricted working space.

In the many applications, however, the controlled quantity is quite often unavailable for direct measurement what may be a significant impediment to effectively apply the ILC, e.g., when some spatial area is inaccessible to measurement transducers or we have to control the state of the DPS in hand via indirect observations of its output. In such a way, the reliability of model predictions is sometimes more important than the accuracy of model parameters, because the ultimate objective in control and modelling is the prediction or forecast of the system states

The control objective is to modify the input signal vector $\mathbf{u}_k(t)$ in each subsequent trial in order to make the measurement output vector $\mathbf{z}_k(t) = [z_k^1(t), \dots, z_k^n(t)]^\top$ follow some differentiable reference trajectory $\mathbf{z}_{\text{ref}}(t)$ with arbitrary accuracy. In this way, it is expected to improve the tracking error norm iteratively in the trial domain:

$$\|\mathbf{e}_k(t)\| = \|\mathbf{z}_k(t) - \mathbf{z}_{\text{ref}}(t)\|$$

i.e. to converge uniformly as close to zero as possible when $k \rightarrow \infty$.

Here, to achieve this control goal we adopt a feedforward ILC scheme, where measurement data gathered at the previous trial can be effectively used to update the control input based on the tracking error [3, 19, 22]. Taking into account a specificity of the dynamics of DPS in context (??)–(??) we propose to apply the following control update:

$$\mathbf{u}_{k+1}(t) = \mathbf{u}_k(t) + \mathbf{\Lambda}_k \dot{\mathbf{e}}_k(t) + \mathbf{\Upsilon}_k \mathbf{e}_k(t) \quad (6)$$

where $\mathbf{\Lambda}_k, \mathbf{\Upsilon}_k \in R^{m \times n}$ are learning coefficients matrices. Such update rule keeps the control design on relatively simple level on one hand, and provides efficient reaction on information included in tracking error on the other hand. Thus, we are flexible in choosing the proper source of learning information:

- the anticipatory update for $\mathbf{\Upsilon}_k = 0$ (so called D-type update rule),
- the proportional update for $\mathbf{\Lambda}_k = 0$ (so called P-type update rule),

in order to speed up the convergence.

2.3 Optimal sensor location

The purpose of the selected measurement strategy is to find such a subset of measurement points to estimate the parameters vector θ of the selected DPS with the greatest possible accuracy in each trail. The effect of this procedure is to be able to estimate the value of the point measurement $q(x, t; \theta)$ from the measurement prohibited zone. Such a zone may, for example, be inaccessible to the sensor by being covered with tool elements or by a restricted working space. For this reason, we are interested in such a subset of measurement points that leads to the maximization of the accuracy of q mapping, hence the choice of the method presented in [28], assuming that the sensors are not mobile. Therefore, the variance of q for the assumed initial parameter vector θ^0 has the form

$$\begin{aligned} \text{var}(q(t; \hat{\theta})) &= \text{E} \left\{ [q(t; \theta) - q(t; \hat{\theta})]^2 \right\} \\ &\approx \frac{\partial q(t; \theta^0)}{\partial \theta} \text{cov}(\hat{\theta}) \left(\frac{\partial q(t; \theta^0)}{\partial \theta} \right)^\top. \end{aligned} \quad (7)$$

It is worth mentioning that in each subsequent iteration the initial vector of θ^0 parameters is equal to $\hat{\theta}$ from the last trial. Under certain assumptions, $\text{cov}(\hat{\theta})$ can be approximated using the inverse of the Fisher's Information Matrix (FIM), which can be represented as

$$M(s) = \frac{1}{Nt_f} \sum_{j=1}^N \sum_{t=0}^{t_f} g(x^j, t) g^\top(x^j, t), \quad (8)$$

where N is number of spatial points and $s(t)$ has following form

$$s = (x^1, x^2, \dots, x^N). \quad (9)$$

The function $g(x, t)$, on the other hand, is a partial derivative with respect to the parameters

$$g(x, t) = \left(\frac{\partial y(x, t; \theta^0)}{\partial \theta} \right)^\top. \quad (10)$$

Hence, on the basis of the equations x and y , we consequently obtained

$$\text{var}(q(t; \hat{\theta})) \sim \frac{\partial q(t; \theta^0)}{\partial \theta} M^{-1}(s) \left(\frac{\partial q(t; \theta^0)}{\partial \theta} \right)^\top. \quad (11)$$

In order to determine the sensor subset that maximizes information about the process, the following objective function should be minimized

$$J = \min \text{tr} \{A(t) M^{-1}(s)\} \quad (12)$$

where

$$A(t) = \left(\frac{\partial q(t; \theta^0)}{\partial \theta} \right)^\top \frac{\partial q(t; \theta^0)}{\partial \theta}. \quad (13)$$

2.4 Clusterization-Free Design for choosing sensors locations

In order to minimize the mentioned objective function, a modification of the so-called clusterization-free scanning. This method consists in exchanging points from a spatial grid between two subsets of \mathcal{Q} one to one. The assumption is that the entire set of measurement points has been divided into two parts. The first subset \mathcal{X}_1 includes a predetermined number of measurements, while the second one \mathcal{X}_2 is its complement. In the spirit of this strategy, the variance $\text{var}(q(t; \hat{\theta}))$ is computed for each point on the spatial grid. Then, elements in each of the members are selected based on the set. For \mathcal{X}_1 the representative will be the point with the greatest variance, while for \mathcal{X}_2 the point with the smallest variance. The condition for the exchange is the fulfillment of the condition of minimizing the variance for a measurement set with some assumed ϵ . The algorithm ends after obtaining the lowest variance for \mathcal{X}_1 or when it reaches the given number of iterations.

3 NUMERICAL EXAMPLE

Let us consider a process of friction welding of two aluminium plates shown in the figure 1. Two symmetrically arranged plates with a thickness of 12.7 mm are welded. The rotating arm and pin of the tool touch the surfaces of both aluminium plates, giving off heat to both. The tool

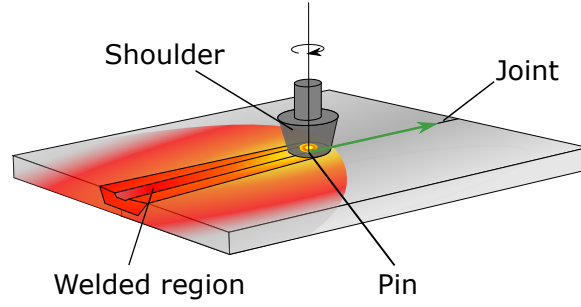


Figure 1: Friction stir welding of an aluminum plate - explanatory figure

moves in a uniform, rectilinear motion along the joint of the plates, creating an assumed uniform weld. To simplify the model, the coordinate system is movable and its origin is at the centre of the pin. In addition to said transformation, it is also assumed that said plates are infinitely long. Such a procedure allows omitting the analysis of the influence of the emission from the edge surface on the thermal processes. Another simplification is the neglect of the mass flow of the melted material. Due to the computational complexity and the assumed symmetry of the system, the area of consideration was also limited to one board. The upper surface of the aluminum is responsible for the natural convection and radiation of the surface to the environment, and the side surfaces are insulated.

Based on the process modelling assumptions presented above, the equation takes the following form:

$$\begin{aligned} \rho C_p \frac{\partial \bar{y}(x, t)}{\partial t} + \rho C_p v(x) \cdot \nabla \bar{y}(x, t) \\ - \nabla \cdot \kappa \nabla \bar{y}(x, t) = 0, \end{aligned} \quad (14)$$

where κ represents thermal conductivity equal $238[W/(mK)]$, $\rho = 2700[kg/m^3]$ is the density, $C_p = 900[J/(kgK)]$ denotes specific heat capacity, and $v(x)$ is the linear speed of the tool along the x-axis. The speed value is fixed at $1.6[mm/s]$ in the opposite direction to the pin movement.

The heat source is generated as the friction of the pin and tool shoulder against the workpiece. These impacts can be considered separately by creating the following relationships:

$$q_p(T) = \frac{\mu}{\sqrt{3(1 + \mu^2)}} r_p \omega(t) \bar{Y}(T), \quad (15)$$

$$q_s(r, T) = \begin{cases} \mu(F_n/A_s)\omega(t)r(x), & \text{if } T < T_{melt} \\ 0, & \text{if } T \geq T_{melt}, \end{cases} \quad (16)$$

where $\mu = 0.4$ is the friction coefficient, $r_p = 6[mm]$ denotes the pin radius, ω is the angular velocity of the pin, $\bar{Y}(T)$ refers to average shear stress of aluminium approximated by the equation $\bar{Y}(T) = 229/(1 + \exp(1/30(T - 465))) + 12[MPa]$ shown in Fig.2, $F_n = 16[kN]$ is the normal force, $A_s = 0.0018504[m^2]$ represents the shoulder surface area and $T_{melt} = 933K$ is aluminium melting temperature. r denotes distance in xy -plane from tool center axis.

Both the lower and upper surfaces emit thermal radiation and natural convection, which is the same as the heat loss of aluminum plates. They can be modeled as two separate heat fluxes:

$$q_u(T) = h_u(T_0 - T + \sigma\epsilon(T_{amb}^4 - T^4)), \quad (17)$$

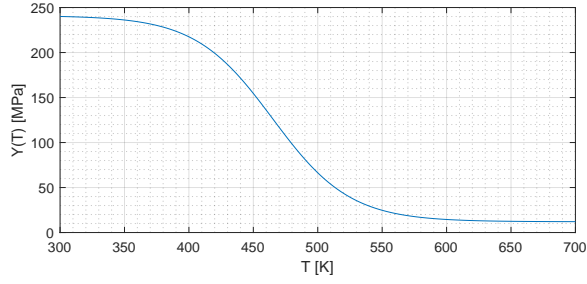
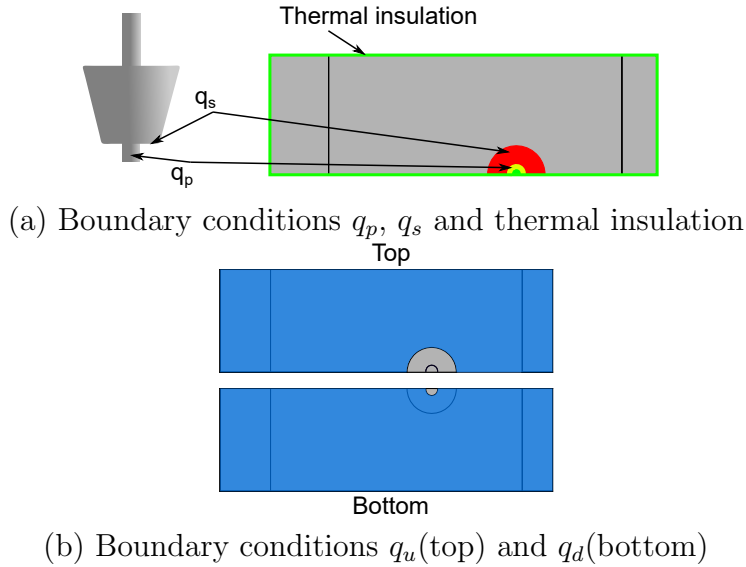


Figure 2: Approximation of $\bar{Y}(T)$

$$q_d(T) = h_d(T_0 - T + \sigma\epsilon(T_{amb}^4 - T^4)) \quad (18)$$

here $h_u = 12.25W/(m^2K)$ and $h_d = 6.25W/(m^2K)$ denote heat transfer coefficient for natural convection, T_0 refers to associated reference temperature ($300K$), ϵ is the surface emissivity, σ is the Stefan-Boltzmann constant and $T_{amb} = 300K$ denotes ambient temperature. To illustrate the



(a) Boundary conditions q_p , q_s and thermal insulation

Top

Bottom

(b) Boundary conditions q_u (top) and q_d (bottom)

Figure 3: Illustration of boundary conditions.

problem of boundary conditions, Fig. 3 shows their graphical interpretation. Fig. 3(a) shows the boundary conditions related to the effect of the actuator on the aluminium plates and the conditions related to the thermal insulation. On the other hand, on fig 3(b) can be seen the conditions related to the emissivity of the surface to the environment from the upper and lower surfaces of the plate, respectively.

The purpose of the control is to follow the reference temperature profile at the selected point.

$$z_{ref}(t) = 633/(1 + \exp(-t + 7.5)) + 300, \quad (19)$$

Moreover, in order to melt the material, the arm and the pin have to generate the appropriate temperature by friction, it is not possible to simply measure the temperature under the tool. Measurement of the temperature at the point located under the tool arm on the upper surface

of the plate is not physically possible, therefore the temperature should be estimated first. For this purpose, the equation describing the temperature evolution with respect to the μ parameter was determined using the partial derivative. The form of heat sources and fluxes are described as follow:

$$\frac{\partial q_p(T, \mu)}{\partial \mu} = \left(\frac{\partial \bar{Y}(T, \mu)}{\partial \mu} + \bar{Y}(T, \mu) \right) \frac{\mu \omega(t) r_p}{\sqrt{3(1 + \mu^2)}} - \frac{\mu^2 \omega(t) r_p \bar{Y}(T, \mu)}{\sqrt{3(1 + \mu^2)^3}}, \quad (20)$$

$$\frac{\partial q_s(r, T, \mu)}{\partial \mu} = \begin{cases} (F_n/A_s)\omega(t)r(x), & \text{if } T < T_{melt} \\ 0, & \text{if } T \geq T_{melt}, \end{cases} \quad (21)$$

$$\frac{\partial q_u(T, \mu)}{\partial \mu} = -h_u \left(\frac{\partial T(\mu)}{\partial \mu} + 4\sigma\epsilon T(\mu)^3 \right), \quad (22)$$

$$\frac{\partial q_d(T, \mu)}{\partial \mu} = -h_d \left(\frac{\partial T(\mu)}{\partial \mu} + 4\sigma\epsilon T(\mu)^3 \right) \quad (23)$$

Such a procedure simplifies the determination of the variance, thus allowing us to find the optimal position of the sensors on the spatial grid. The set of these sensors simultaneously enables the estimation of temperature measurements in a forbidden place. Hence it is possible to follow the reference temperature.

The simulations were carried out using a PC with Intel Core i7 1.99 GHz and 16 GB RAM. On the software side, COMSOL MULTIPHISICS 5.4 and MATLAB 2016b were used. The model consists of 668 spatial points and 1758 triangular and quadratic prisms, and 501 time intervals $t \in [0; 50]$. In the figure showing the spatial grid, the area forbidden for measurement, due to the tool operation, and modelling simplifications (such as infinite domains) are marked with light gray. Additionally, a red x-marker indicates a point that is interesting to measure.

It is assumed that the number of sensors participating in the experiment cannot exceed 10% of the points allowed for measurement. At the same time, the greater their number, the more accurate the knowledge about the dynamics of the process. However, there is a limited number at which the quality of information slightly improves. The following shows how the position of the measurement points changes during the first iteration (from blue to green). First, a set of input points is drawn. Then, to find the minimum variance, clustering-free scanning is used. As you can see in the figure 6 the set change its points (green points). Interestingly, from an engineering point of view, it would seem that the best solution to obtain the best information about the process should be to distribute the measurement grid evenly. However, what can be seen about the dynamics of the process can be found by taking measurements near the forbidden zone. This is due to the fact that the friction parameter μ affects the tool environment. In a similar experiment, when the parameters describing the emissivity were taken into account, the measurement could be moved to another area. It is strongly related to the distribution of ratios described by derivative instruments in terms of parameters (see Fig. 7). Determining the place of measurement is not an obvious task as mentioned above, on the contrary, it is a non-trivial task that often requires solving very difficult equations with often very conservative assumptions.

An experiment scenario was assumed that shows the influence of the number of parameters as indicators used in the measurement strategy. Table x proposes combinations of parameters and

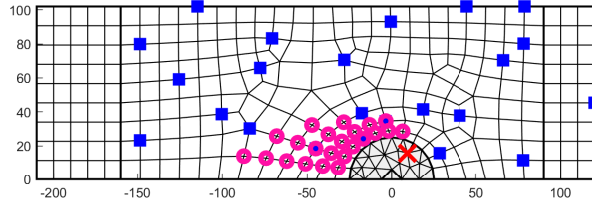


Figure 4: Search for optimal measurement points for μ .

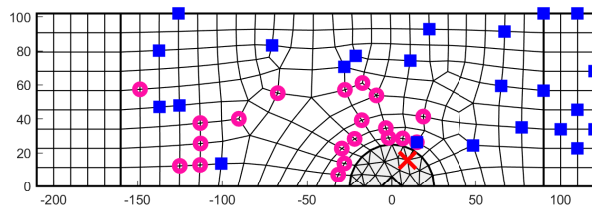


Figure 5: Search for optimal measurement points for μ and h_u .

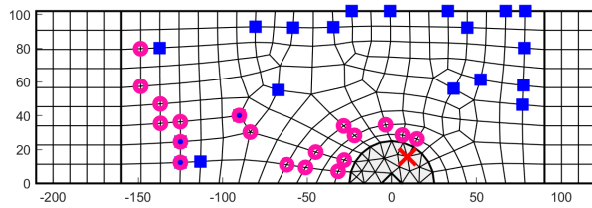


Figure 6: Search for optimal measurement points for μ , h_u and h_d .

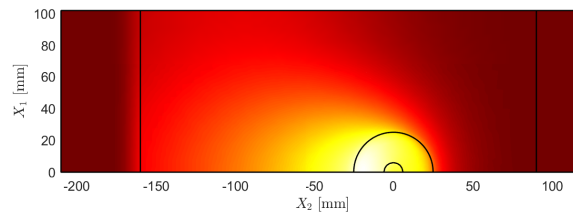


Figure 7: Distribution of μ .

Parameters	MSE for last iteration
μ	0.60430
μ, h_u	0.01213
μ, h_u, h_d	0.01215

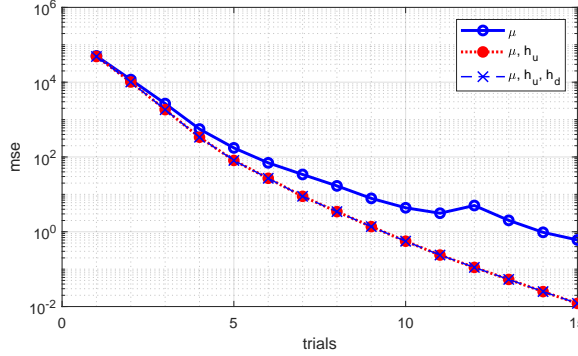


Figure 8: Convergence of ILC

the mean square errors obtained for them from the last ILC trials. Such a comparison can clearly demonstrate the quality of the estimation in terms of the number and selection of parameters.

The next step is to determine the value of the parameters for the model estimating the temperature at the point from the forbidden zone. Using mentioned measurement strategy it is possible to find a parameters that allow a fairly accurate temperature estimation in chosen point. In order to obtain the melting point of aluminium allowing for welding of two plates, the tool rotational speed was used as a control value, while the tuning of this value was taken over by the control algorithm with iterative learning of the P-type.

In order to confirm the correctness of choosing the parameters and their number, an analysis of the convergence of the ILC algorithm with a constant learning coefficient $\lambda = 0.256$ determined using optimization methods was performed, the results are shown in Fig. 8. As can be seen, in the case of a single parameter in the form of the friction coefficient, there is a tendency to minimize the error. However, the use of additional information related to the emissivity from the top surface h_u improves the estimation of the measurement value and at the same time translates into acceleration and improvement of convergence. Moreover, the use of the third piece of information, which at the same time has the smallest impact on the measurement at the point of interest to us, does not significantly improve the convergence rate, but also slightly worsens it.

For this reason, the best version with two parameters was adopted in further consideration. As can be seen in Fig. 9, the evolution of temperature for subsequent selected trials is presented. Already on the fifth trial, the algorithm begins to do very well with trajectory tracking. It is worth noting that the error in the last iteration is only less than 0.11 [K] which is much less than 0.1%. It is also worth noting that despite the large overshoot of 43%, the maximum rotational speed is significantly lower than the permissible rotational speeds for spindles in such applications, permissible in the literature

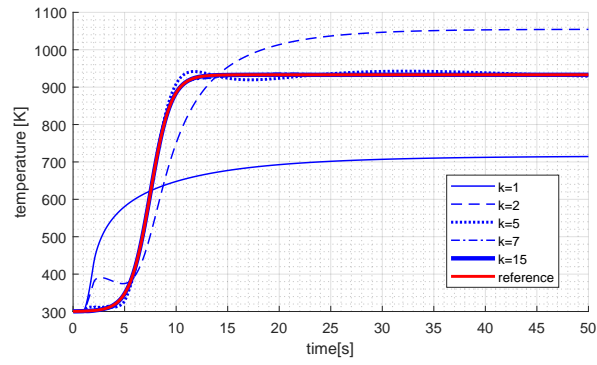


Figure 9: Temperature in trials.

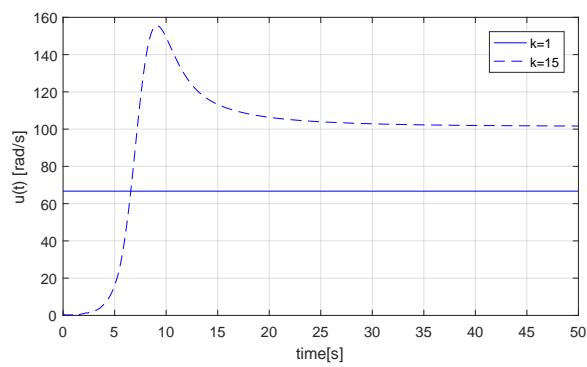


Figure 10: Control signal.

References

- [1] Hyo-Sung Ahn, YangQuan Chen, and Kevin L Moore. Iterative learning control: brief survey and categorization. *IEEE Transactions on Systems Man and Cybernetics Part C Applications and Reviews*, 37(6):1099, 2007.
- [2] William F Ames. *Numerical methods for partial differential equations*. Academic press, 2014.
- [3] Suguru Arimoto, Sadao Kawamura, and Fumio Miyazaki. Bettering operation of robots by learning. *Journal of Robotic systems*, 1(2):123–140, 1984.
- [4] Alain Bensoussan, Giuseppe Da Prato, Michel C Delfour, and Sanjoy K Mitter. *Representation and control of infinite dimensional systems*, volume 1. Birkhäuser Boston, 1992.
- [5] D. A. Bristow, M. Tharayil, and A. G. Alleyne. A survey of iterative learning control: a learning-based method for high-performance tracking control. *IEEE Control Systems Magazine*, 26(3):96–114, 2006.
- [6] Douglas A Bristow, Marina Tharayil, and Andrew G Alleyne. A survey of iterative learning control. *Control Systems, IEEE*, 26(3):96–114, 2006.
- [7] Dan Gabriel Cacuci, Ionel Michael Navon, and Mihaela Ionescu-Bujor. *Computational Methods for Data Evaluation and Assimilation*. CRC, Boca Raton, FL, 2014.
- [8] B. Cichy, K. Galkowski, and E. Rogers. Iterative learning control for spatio-temporal dynamics using Crank–Nicholson discretization. *Multidimensional Systems and Signal Processing*, 23:185–208, 2012.
- [9] Ruth F Curtain and Hans Zwart. *An introduction to infinite-dimensional linear systems theory*, volume 21. Springer Science & Business Media, 2012.
- [10] Xi-Sheng Dai, Xing-Yu Zhou, Sen-Ping Tian, and Hong-Tao Ye. Iterative learning control for mimo singular distributed parameter systems. *IEEE Access*, 5:24094–24104, 2017.
- [11] Valerii V Fedorov and Peter Hackl. *Model-oriented design of experiments*, volume 125. Springer Science & Business Media, 1997.
- [12] Chris T Freeman, Eric Rogers, A Hughes, Jane H Burridge, and Katie L Meadmore. Iterative learning control in health care: electrical stimulation and robotic-assisted upper-limb stroke rehabilitation. *Control Systems, IEEE*, 32(1):18–43, 2012.
- [13] Qin Fu, Panpan Gu, and Jianrong Wu. Iterative learning control for one-dimensional fourth order distributed parameter systems. *Science China Information Sciences*, 60(1):1–13, 2017.
- [14] Deqing Huang, Jian-Xin Xu, Xuefang Li, Chao Xu, and Miao Yu. D-type anticipatory iterative learning control for a class of inhomogeneous heat equations. *Automatica*, 49(8):2397–2408, 2013.
- [15] Werner G. Müller. *Collecting Spatial Data. Optimum Design of Experiments for Random Fields*. Contributions to Statistics. Heidelberg, 3rd revised and extended edition, 2007.

- [16] Sigeru Omatu and John H. Seinfeld. *Distributed Parameter Systems: Theory and Applications*. Oxford Mathematical Monographs. New York, 1989.
- [17] Krzysztof Patan and Maciej Patan. Neural-network-based iterative learning control of non-linear systems. *ISA transactions*, 98:445–453, 2020.
- [18] Maciej Patan. *Optimal sensor networks scheduling in identification of distributed parameter systems*, volume 425. Springer Science & Business Media, 2012.
- [19] Maciej Patan, Kamil Klimkowicz, Robert Maniarski, Krzysztof Patan, and Eric Rogers. Iterative learning control of the displacements of a cantilever beam. In *58th IEEE Conference on Decision and Control, CDC 2019, Nice, France*, page 2019, 5593–5598.
- [20] Maciej Patan, Kamil Klimkowicz, and Krzysztof Patan. Iterative learning control for distributed parameter systems using sensor-actuator network. In *16th International Conference on Control Automation Robotics and Vision, ICARCV 2020*, page 2020, 1200–1205.
- [21] Maciej Patan and Damian Kowalów. Distributed scheduling of measurements in a sensor network for parameter estimation of spatio-temporal systems. *International Journal of Applied Mathematics and Computer Science*, 28(1):39–54, 2018.
- [22] Maciej Patan, Krzysztof Patan, Krzysztof Gałkowski, and Eric Rogers. Iterative learning control of repetitive transverse loads in elastic materials. In *57th IEEE Conference on Decision and Control, CDC 2018, Miami, FL, USA, December 17-19, 2018*, pages 5270–5275, 2018.
- [23] José M Rodríguez, David Sánchez, Gonzalo S Martínez, Badr Ikken, et al. Techno-economic assessment of thermal energy storage solutions for a 1 mwe csp-orc power plant. *Solar Energy*, 140:206–218, 2016.
- [24] Ne-Zheng Sun and Alexander Sun. *Model Calibration and Parameter Estimation For Environmental and Water Resource Systems*. Springer, New York, 2015.
- [25] A Tayebi, S Abdul, MB Zaremba, and Y Ye. Robust iterative learning control design: application to a robot manipulator. *Mechatronics, IEEE/ASME Transactions on*, 13(5):608–613, 2008.
- [26] Christophe Tricaud and YangQuan Chen. *Optimal Mobile Sensing and Actuation Policies in Cyber-physical Systems*. Springer, London, 2012.
- [27] Dariusz Ucinski. *Optimal measurement methods for distributed parameter system identification*. CRC Press, 2004.
- [28] Dariusz Ucinski. *Optimal measurement methods for distributed parameter system identification*. CRC Press, 2004.
- [29] Antonio Yarza, Victor Santibanez, and Javier Moreno-Valenzuela. An adaptive output feedback motion tracking controller for robot manipulators: uniform global asymptotic stability and experimentation. *International Journal of Applied Mathematics and Computer Science*, 23(3):599–611, 2013.